

## Dielectric Properties of Polyethylene Foams at Medium and High Frequencies

Martin Strååt<sup>1</sup>, Igor Chmutin<sup>2</sup> and Antal Boldizar<sup>1</sup>

<sup>1</sup>Chalmers University of Technology, Department of Materials and Manufacturing Technology, Hörsalsv. 7, SE-412 96 Göteborg, Sweden

<sup>2</sup>Institute of Radio Engineering and Electronics, RAS, 1 Vvedenskii Square, Fryazino, Moscow region 141190, Russia.

### ABSTRACT

In modern communication cables, expanded polyethylene (PE) is used as insulation material in order to reduce the signal losses. This work addresses the influence of porosity and cell shape on the dielectric properties of expanded PE. Foams were produced using a single-screw extruder with a slit die. Dielectric spectroscopy revealed improving dielectric properties with increasing porosity at both medium frequencies (34 kHz) and high frequencies (11.2 GHz). The cells were elongated and flat which in combination with increasing porosity resulted in a transition from a parallel equivalent circuit to a series equivalent circuit at about 28% porosity.

### INTRODUCTION

Polyethylene (PE) is widely used for insulation of cables since it has a low dielectric constant ( $\epsilon'$ ) and a low dielectric loss factor ( $\epsilon''$ ). However, above 1 GHz, the dielectric loss factor generally increases with increasing frequency<sup>1</sup>. The maximum rate of data transfer through a cable is determined by the bandwidth and the signal-to-noise ratio<sup>2</sup>, where the noise is dependent on the dielectric loss factor of the foam insulation. Power consumption in a cable transmission line is dependent on the attenuation of the cable which in turn is dependent on both the dielectric constant and the dielectric loss factor of the insulation. Recent and expected

new demands in telecommunications for increased data transfer rates mean that higher frequencies are being necessary and this requires a better understanding of the dielectric properties of insulation materials above 1 GHz. By foaming the material, the dielectric constant and loss factor of the insulation can be lowered, and both theoretical analysis and experimental data indicate that the shape of the gas cells can have a significant influence on the dielectric behaviour<sup>3-5</sup>. The loss factor is primarily lowered when the concentration of hindered permanent dipoles in the material is reduced<sup>6</sup> and, since the permanent dipoles in the gas phase are not hindered, increased foaming can have a diluting effect on the concentration of hindered permanent dipoles.

Models of the dielectric properties of heterogeneous systems (such as foams) are usually defined between an upper limit (Eq. 1), with an equivalent circuit of capacitances and resistances connected in parallel, and a lower limit (Eq. 2 and 3) with an equivalent circuit of capacitances and resistances in series<sup>7</sup>. The upper-limit model for the loss tangent ( $\tan \delta$ ) can be found by replacing  $\epsilon'$  with  $\epsilon''$  in Eq. 1.

$$\epsilon_c' = (1 - v_g) \epsilon_s' + v_g \epsilon_g' \quad (1)$$

$$\varepsilon_c' = \frac{\varepsilon_s' \varepsilon_g'}{\varepsilon_s' v_s + \varepsilon_g' v_g} \quad (2)$$

$$\tan \delta_c = \frac{\tan \delta_s + \frac{\varepsilon_s' v_g}{\varepsilon_g' v_s} \tan \delta_g}{1 + \frac{\varepsilon_s' v_g}{\varepsilon_g' v_s}} \quad (3)$$

where  $\varepsilon'$  is the dielectric constant,  $\tan \delta$  is the loss tangent and  $v$  is the volume fraction,  $c$  refers to the composite,  $s$  to the solid phase and  $g$  to the gas phase.

The two-layer capacitor model (connection in series) is one of the simplest models for a composite dielectric and it is a reasonable approximation for embedded flakes oriented perpendicular to the field<sup>3</sup>. With embedded rods, an intermediate model giving predictions between those of the parallel equivalent circuit and those of the series equivalent circuit is sometimes used. However, materials with a low concentration of inclusions can also be represented by the parallel model<sup>5</sup> unless the inclusions are exceptionally flat. If the inclusions, such as gas cells, are flattened out in a direction perpendicular to the applied electric field, their dielectric behaviour can be represented by a two-layer capacitor<sup>3</sup> and Eq. 2 is then more appropriate.

Factors that strongly influence the dielectric losses are interfacial polarisation, dipoles present in the material and frequency<sup>1,4</sup>. The effects of these factors are however not easy to separate in a low-loss material and it is thus not easy to establish useful relations between the dielectric loss factor and the cell geometry in such materials. Studies of the influence of cell geometry and porosity on the dielectric properties of various systems are described in a comprehensive review by Van Beek<sup>7</sup>. The models proposed are generally valid only within a certain range of porosities and for materials with very large differences in dielectric properties. The influence of

frequency depends on the loss mechanism where the loss factor generally reaches a peak value at a certain frequency. Several mechanisms can coexist but the resulting loss factor can be described by a universal model (Eq. 4) as shown by Jonscher<sup>8</sup>.

$$\frac{1}{\chi''} = \left( \frac{\omega}{\omega_2} \right)^{-m} + \left( \frac{\omega}{\omega_1} \right)^{1-n} \quad (4)$$

where  $\chi''$  is the measured dielectric loss,  $\omega$  is angular frequency,  $\omega_2$  and  $\omega_1$  are peak angular frequencies and  $m$  and  $n$  are curve fitting parameters.

Foam extrusion rarely yields perfectly spherical cells. Haul-off units, die walls, temperature gradients and changes in the melt flow rate usually affect the final cell structure<sup>9</sup>. A deeper understanding of how the cell shape can influence  $\varepsilon'$  and  $\varepsilon''$  could thus help to achieve low dielectric losses in foamed structures. This study aims to clarify the relationships between the dielectric properties and the foaming conditions for extruded foams prepared using commercial polymer blends.

## EXPERIMENTAL

### Materials

Two commercial PE grades were used, one high density polyethylene (HDPE), named HE3366, with density 945 kg/m<sup>3</sup> and melt flow rate (MFR) 0.7 g/10min (190°C, 2.16 kg) and one low density polyethylene (LDPE), named LE1800, with density 922 kg/m<sup>3</sup> and MFR 1.9 g/10min (190°C, 2.16 kg), both supplied by Borealis A/S. Two blends of HDPE and LDPE were made where 85% HDPE and 15% LDPE, by weight, was denoted HPE and equal amounts of HDPE and LDPE was denoted MPE. All the materials also contained 0.5% of standard oxidation stabilising additives, according to the supplier. Approximately 0.5% of azodicarbonamide was added to the blends as a chemical blowing agent (CBA).

Equivalent mixtures of HDPE and LDPE, without foaming agent, corresponding to the HPE and MPE materials, called HPE-eq and MPE-eq were also prepared.

### Extrusion

Foams were extruded using a slit die mounted on a single screw laboratory extruder, Brabender model E 19/25D. The screw used was a standard metering screw with a diameter of 19 mm, a length/diameter (L/D) ratio of 25 and a compression ratio of 4:1. The slit die had a width of 100 mm, an adjustable height between 0 and 1.5 mm and a land length of 25 mm. A haul-off unit was used, type Brabender Univex, consisting of a system of temperature controlled steel rolls with adjustable nip pressure. The rolls were 98.5 mm in diameter and 200 mm wide. By adjusting the haul-off rate between 0.18 and 0.40 m/min, the distance from the die to the rolls from 76 mm to 150 mm and the nip pressure, it was possible to obtain extrudates with different cell shapes and porosities. The temperature settings of the extruder used in order to obtain foamed sheets with different densities were, starting from the material feed, 185°C, 195°C and 205°C. Rotational speeds were varied from 10 rpm to 60 rpm. Azodicarbonamide decomposes at about 195°C<sup>10</sup> and, in order to ensure efficient use of the blowing agent, the temperature was kept above 200°C in zone 3 of the extruder. A higher and a lower temperature in the third zone were also tried. The die temperature was varied between 190°C and 210°C in order to study the extensional properties of the melt. The foams used for studying the cell shapes were produced with the temperature settings mentioned above, a screw rotational speed of 40 rpm, giving a mass flow rate of 16 g/min, a haul-off rate of 0.27 m/min and a nip line pressure of 1 N/cm.

The density of produced foams was measured gravimetrically according to ASTM standards D 792 and D 1622.

### Capillary viscometer measurements

Equivalent blends of HPE and MPE (without the CBA) were prepared by melt mixing in a Brabender mixing chamber, model AEV 330. The compounding was performed at a rotational speed of 30 rpm at 190°C for 5 minutes. The extensional flow behaviour of HPE-eq and MPE-eq was measured using a capillary viscometer type Rheoscope 1000, Ceast 6742/000 equipped with a Rheotens attachment. The temperatures used were 190°C and 210°C, the capillary had a length ( $L$ ) of 10 mm and a diameter ( $D$ ) of 1 mm. The elongational properties were estimated using the uniaxial extension method as described by Acierno and La Mantia<sup>11</sup>. In this method, the strand extruded from the capillary is picked up by a rotating wheel, positioned below the exit of the capillary, which stretches the strand and enables the stress-strain behaviour of the melt to be determined. The strain in the strand was evaluated from the difference between the tangential velocity of the rotating wheel and the velocity of the extruded strand, the latter being kept at 17 mm/s. During the experiments, the velocity of the rotating wheel was accelerated at a rate of 1 mm/s<sup>2</sup> with a starting velocity of 17 mm/s, in order to increasingly stretch the extruded strand. The force required to stretch the melt was measured with a transducer. The measurements were not isothermal as the stretching took place after the exit from the capillary, but this is not expected to affect the main conclusions arrived at here.

### Dielectric measurements

The dielectric properties  $\epsilon'$  and  $\epsilon''$  were measured using two instruments. For frequencies below 1 MHz, a broadband, high-resolution dielectric spectrometer, made by Novocontrol was used with a type Alpha-A analyser and a sample cell using brass parallel plate electrodes with a diameter of 25 mm<sup>12</sup>. A similar broadband dielectric spectrometer, model BDS40 also

made by Novocontrol with a similar setup was used to evaluate the frequency dependence of specimens slightly oxidised in air using radiation. The oxidation was made to increase the signal-to-noise ratio. The thickness of the specimens was typically around 1 mm and was measured using a micrometer giving the thickness measurement an accuracy of approximately  $\pm 0.5\%$ . Measurements with this instrument were performed at room temperature by scanning from 10 Hz to 1 MHz, although reliable data for the samples could only be obtained in the frequency range from 600 Hz to 34 kHz. The instrument could determine the ratio  $\varepsilon''/\varepsilon'$ , also called  $\tan \delta$ , with an accuracy of the order of 30  $\mu\text{rad}$  (with regard to the phase angle  $\delta$ ) according to manufacturer specifications. The specimens were dried in an oven at either 60°C or 80°C for 16 h prior to measurement in order to reduce the influence of water.

For measurements at frequencies higher than 1 GHz, the resonance waveguide method was used as described by Rozhkov<sup>13</sup>. The waveguide was a cavity resonator with a rectangular parallelepiped interior geometry of 36mm x 15 mm x 10 mm. The internal surfaces were coated with silver. Samples were cut from the sheets, 15 mm long and 3 mm wide with a thickness of approximately 1 mm as described earlier in this section. A single frequency of 11.2 GHz was used in the present case. The experimental scatter at this frequency was rather high, amounting to 25-33%, mainly related to the arrangement of the sample in the measuring chamber and to some uncertainty in the determination of the specimen volume.

### Optical microscopy

A Leica MZ12 microscope equipped with a digital camera, Olympus DP11, was used to determine cell size, aspect ratio and orientation. The specimens were cut from the mid-section of the extruded sheets. The

length-to-width ratio of the cells was taken as the shape factor of the cells.

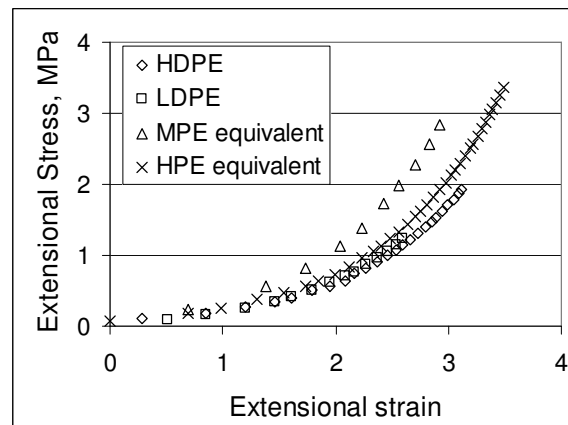
## RESULTS

### Extensional flow behaviour

As can be seen in Fig. 1, the stress required to achieve a given strain was higher with MPE-eq than with HDPE at 190°C over the studied range of extensional strain. The extensional strain (Eq. 5) is calculated as

$$\lambda = \ln\left(\frac{v_1}{v_0}\right) \quad (5)$$

where  $\lambda$  is the extensional strain,  $v_1$  is the speed at the pick-up wheel and  $v_0$  is the extrusion speed<sup>11</sup>. Close to the strain-at-break, approximately 50% higher stress was needed which indicates a substantial strain hardening behaviour. For HPE-eq at the same temperature, the strain hardening was about 20% higher than that of the HDPE<sup>14</sup>. The strain at break of HPE-eq was significantly higher than for the other materials studied. At 210°C, no significant difference in strain hardening was observed between the materials.



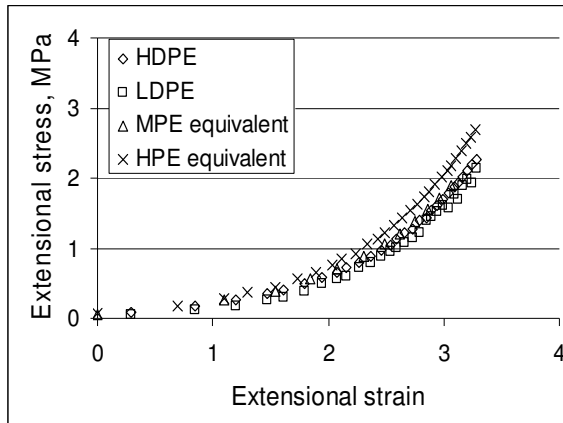


Figure 1. The extensional properties at 190°C (top) and 210°C (bottom) measured with the Rheotens method.

### Microscopy of foamed sheets

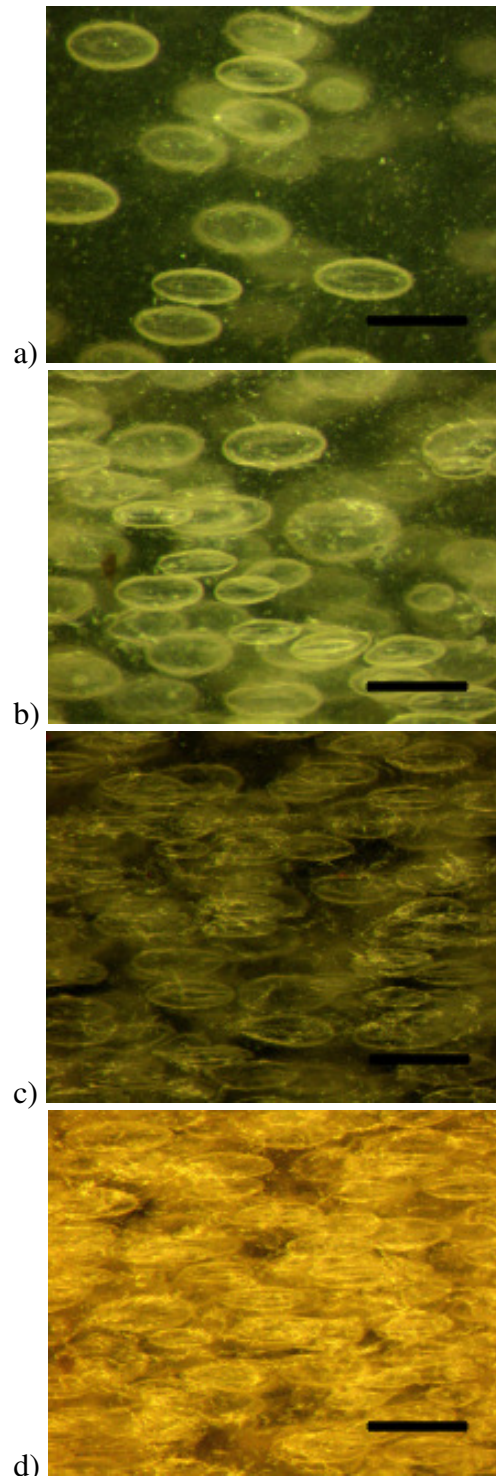
The cell size and the cell shape of some selected foams were assessed by optical microscopy, see Fig. 2. The cells were elongated in the flow direction, increasing die temperature leading to increasing porosity and increasing elongation. For similar process conditions, porosity and cell density were higher in HPE than in MPE and there was a tendency towards smaller cells at higher porosities.

The mean thickness of cells was estimated to be below 100  $\mu\text{m}$  for foams produced with a high screw speed and with the haul-off unit close to the die. The length/width/thickness ratios were typically about 5: 2:1 respectively.

### Dielectric properties of foamed sheets

The dielectric losses at frequencies of 34 kHz and 600 Hz are shown in Table 1 for specimens of different porosities and different drying temperatures. An increase in the drying temperature from 60°C to 80°C led to a significantly higher  $\epsilon''$ , especially at the lower frequencies. At a given frequency, the  $\epsilon''$  -values decreased with increasing porosity up to a porosity of 43% (higher porosities were achieved with a different die), as shown in Fig. 3 for a frequency of 34 kHz. The quite pronounced increase in the

dielectric loss factor when 0.5% CBA was added is also evident in Fig. 3.



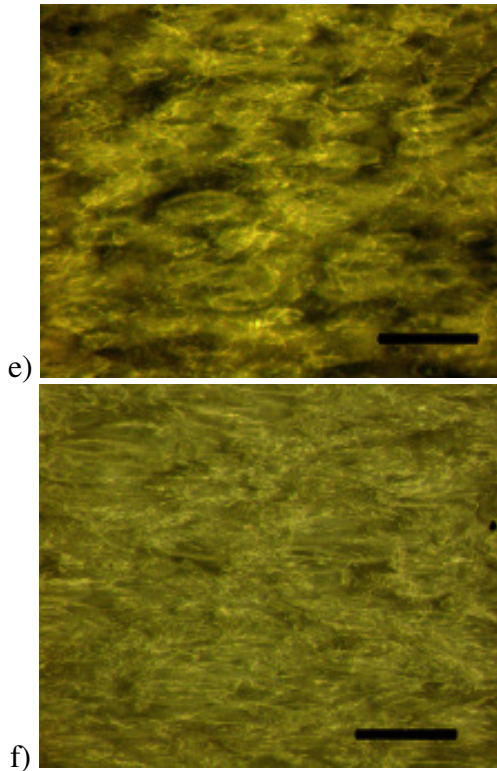


Figure 2. Optical micrographs showing the cell structure of foams, viewed in the through-thickness direction. The die temperature and the porosity are given for each material. For MPE materials: a) 200°C, 5%, b) 205°C, 10%, c) 210°C, 21%, d) 210°C, temperature at screw tip increased to 210°C, 28%. For HPE materials: e) 205°C, 30%, f) 210°C, temperature at screw tip increased to 210°C, 43%. Scale bar represents 500  $\mu\text{m}$ .

Fig. 4 shows that the dielectric constant  $\epsilon'$  decreased with increasing porosity. The upper and lower bounds defined earlier (Eq. 1 and 2) are also included in the graph. At a certain porosity (around 40%), a transition seemed to take place from an upper-bound to a lower-bound behaviour. It may be reasonable to assume that this transition depends on the porosity and on the shape factor and that increasing both shape factor and porosity leads to a near two-layer behaviour, the lower-bound behaviour being modelled as a two-layer material. That a lower dielectric constant at a given porosity

can be achieved with flat cells has been reported by other authors<sup>3,15</sup>. A more detailed study is required to substantiate the onset of the transition seen. Behaviour similar to that shown in Fig. 3 was observed over the frequency range 600 - 34000 Hz.

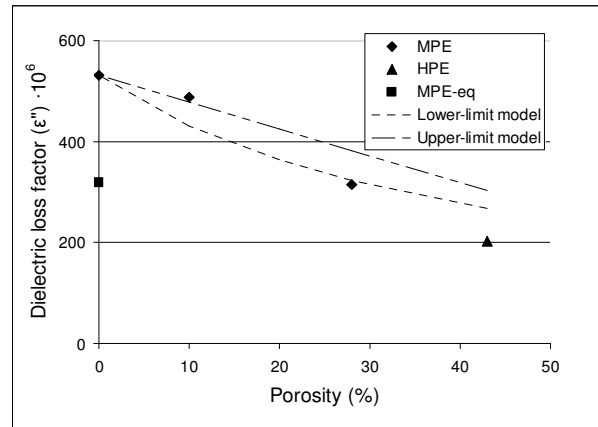


Figure 3. The dielectric loss factor at 34 kHz as a function of porosity for the PE specimens in Table 1. Models were based on the measured value of unexpanded MPE (with CBA).

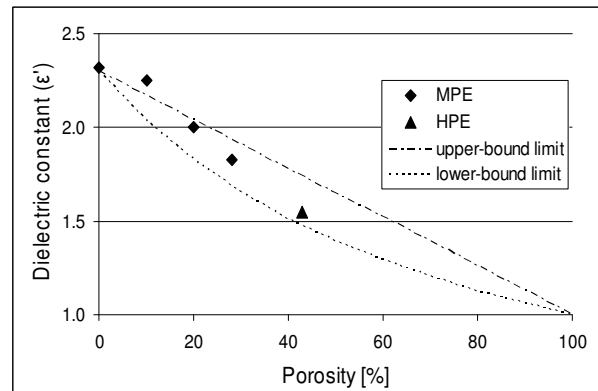


Figure 4. The dielectric constant of foams at 34 kHz seen in Table 1. The upper limit is represented by an equivalent circuit of capacitors in parallel and the lower limit corresponds to an equivalent circuit of capacitors in series.

The dielectric loss factor should also be affected by a transition to a two-layer behaviour since  $\epsilon'$  and  $\epsilon''$  are coupled<sup>1,7</sup>. This may however have been obscured by

the polar residues from the CBA which lead to a twofold increase in the  $\epsilon''$  value compared to a similar material without CBA.

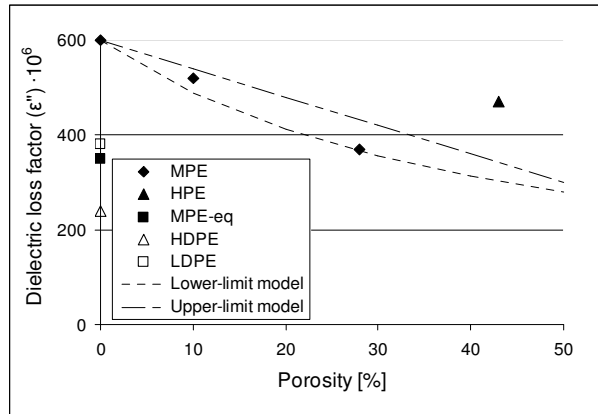


Figure 5. The dielectric loss factor vs porosity of PE specimens measured at 11.2 GHz. Specimens were kept for 4 weeks at room temperature in a dry atmosphere in order to reduce the moisture content.

At the higher frequency 11.2 GHz, the dielectric loss factor, shown in Fig. 5, exhibited a similar behaviour to that shown in Fig. 3. Again,  $\epsilon''$  decreased in general with increasing porosity and the negative effect of the CBA was obvious. The magnitudes of  $\epsilon''$  at 34 kHz and 11.2 GHz were quite similar, and the lowest  $\epsilon''$ -value was obtained with the HDPE that contained no chemical blowing agent (CBA), as concluded by Bur<sup>1</sup>. The dielectric constant

decreased with increasing porosity at 11.2 GHz without exhibiting the transition seen in Fig. 4.

The frequency dependency of the dielectric losses is shown in Fig. 6. The relative reduction of foamed MPE compared with solid MPE was found to be more or less constant over the frequency range. Foaming also influenced the peak frequencies, calculated with Eq. 4, increasing porosity leading to decreasing peak frequency.

## DISCUSSION

The extensional strain hardening of the melt is usually very important during the expansion and solidifying stages of extrusion foaming<sup>16</sup>. Fig. 1 clearly shows that the melts had a lower resistance to deformation at the higher temperature. The strain at break in all samples was high, as expected for these materials<sup>10</sup>. Assuming that the melt is not strained to the strain at break during foam growth, a high elongational viscosity may be expected to result in a low porosity and insufficient growth rate, as seen in Fig. 2, whereas a low elongational viscosity would be expected to promote rapid growth but also cell wall rupture and coalescence of cells, see Fig. 2. By maintaining (and adjusting) the temperature of the die between 200°C and

Table 1. The porosity and dielectric properties of some selected foams at 600 Hz and 34 kHz. Samples were dried for 16 h prior to measurement, the drying temperature is indicated as a subscript in  $\epsilon''$ .

Material	HPE	MPE	MPE	MPE	MPE	MPE-eq	HPE	MPE	MPE	MPE	MPE	MPE-eq
Frequency, kHz	34	34	34	34	34	34	0.6	0.6	0.6	0.6	0.6	0.6
Porosity, %	43	28	20	10	0	0	43	28	20	10	0	0
$\epsilon'$	1.55	1.83	2.00	2.25	2.32	2.30	1.55	1.83	2.00	2.25	2.32	2.30
$\epsilon''_{60^\circ\text{C}} \cdot 10^6$	202	314	-	487	531	319	316	423	-	689	1030	299
$\epsilon''_{80^\circ\text{C}} \cdot 10^6$	317	350	481	599	624	-	629	716	862	1020	1120	-

Table 2. The porosity and dielectric properties of the foams at 11.2 GHz. Specimens were kept 4 weeks in a dry atmosphere prior to measurement.

Material	HPE	MPE	MPE	MPE	MPE-eq	HDPE	LDPE
Porosity, %	43	28	10	0	0	0	0
$\epsilon'$	1.68	1.79	2.02	2.20	2.20	2.20	2.24
$\epsilon'' \cdot 10^6$	470	370	520	600	350	240	380

210°C, the rate of growth of the cells could be controlled to produce foams with different cell shapes.

Specimens dried at 80°C for 16 h was observed to have increased dielectric losses, likely due to the formation of short side chain branches such as carbonyls in the material which increased the dielectric losses<sup>3</sup>.

Using the data in Fig. 6 to calculate the influence of porosity on dielectric loss factor, according to Eq. 3, resulted in lower losses than predicted with the upper-limit

and lower-limit models. The loss tangent of the gas phase was assumed to be very small and the loss tangent of the solid phase was assumed to be equal to the MPE with 0% porosity. However, if the curves were to be shifted so that the peaks coincide at the same frequency the data would have a fair correlation with the lower-limit model.

The increase in dielectric loss factor in the foamed blends, Fig. 3 and 5, compared with the equivalent blends with no CBA, is according to our results strongly correlated with permanent dipoles from the CBA, still

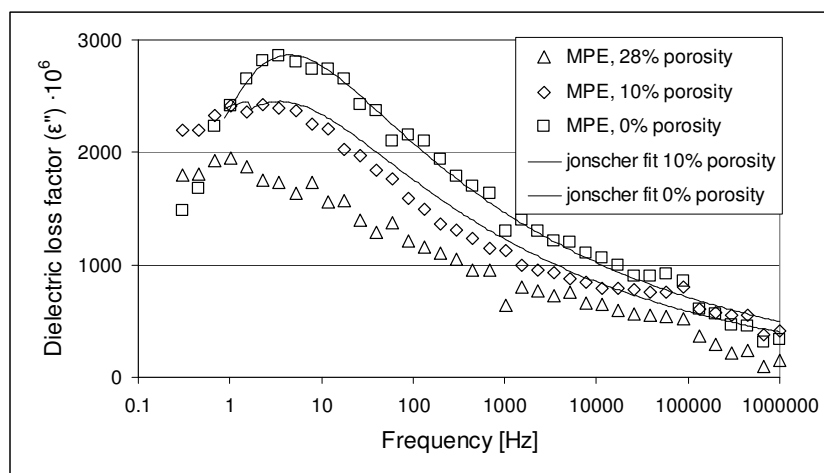


Figure 6. Dielectric loss factor plotted vs frequency for MPE specimens slightly oxidised in air using radiation.

present in the melt after activation of the CBA. In Fig. 5, the foam with 43% porosity was made using HPE where the concentration of CBA was actually determined to be 0.6%, which was 0.1% higher than for MPE. This could be one reason why it exhibited a relatively high loss factor. Our results clearly shows that small amounts of CBA in a PE blend does not

change the dielectric constant of the material in a significant way, see Tables 1 and 2.

The results presented in fig 4 indicate the existence of a transition towards the lower-bound limit, which could however not be seen at the higher frequency in Fig. 6. However, it is possible that the specimens were oxidized prior to measurement which would have decreased the resistivity of the cell walls. With decreased resistivity of the

cell walls, the lower-bound model is not applicable. The lower-limit model is believed to be correct for polymer foams with flat cells under the assumption that the resistivity of the polymer is very high<sup>3</sup>. It is therefore possible that the shape of the cells could reduce the dielectric constant at higher porosities compared with the prediction of the upper-limit model<sup>15</sup>. The indication in Fig. 4 points to the possibility of achieving a structure with improved dielectric properties using commonly available polymer blends and foam processing techniques.

As a combination of cell structure and porosity significantly reduced both the dielectric loss factor, Fig. 3 and Fig. 5, and the dielectric constant, Fig. 4, it was important to try to correlate this behaviour in some way with the processing of the material. The elongational properties of the PE blends were found to correlate well with earlier studies by Acierno and La mantia<sup>14</sup> performed on similar materials using the same type of equipment.

The elongated shape of the cells results from the consolidation in a stretching flow in the flow region from the die to the haul-off unit. The strain-hardening properties of the melt restricted thinning and rupture of the cell walls, thus reducing both cell elongation and cell growth. As a result, the material which showed more strain-hardening behaviour (MPE) was easier to process, and the final structure was easier to control. A disadvantage with strain hardening was, however, that the material would not reach high porosities.

Flattening of the cells is dependent on the stress relaxation properties of the melt, the nip pressure and the residence time. As the foamed melt passed through the haul-off unit, cells were further flattened and elongated which in turn led to an increased overlapping of cells, promoting a lower-limit (two-layer) dielectric behaviour. Cells produced with MPE showed a lower porosity, lower stretching and less coalescence compared with the cells

produced with the HPE, which showed less strain hardening.

The MPE foam with 5% porosity in Fig. 2 can not be expected to behave like a two-layer dielectric since overlapping of cells is scarce. The MPE foam with 28% porosity on the other hand shows cell overlapping and is likely to behave like a two-layer dielectric. It seems probable that a transition occurs from an upper-bound limit to a lower-bound limit over a certain range of porosities and that the point of onset of the transition depends on the cell shape.

## CONCLUSIONS

The dielectric constant of foamed polyethylene blends depends on the porosity and on the cell shape, as has been reported by others. With a low-loss matrix material and cells shaped like ellipsoids oriented perpendicular to the field there was an indication of a transition from the upper-bound limit of the dielectric constant towards the lower-bound limit, represented by the two-layer dielectric model, when the porosity was increased. The dielectric loss factor of foams decreased with increasing porosity although the detailed relationship between these quantities is yet to be established.

Post-extrusion operations changed the shape of cells in a way that could lead to an almost two-layer dielectric behaviour of the material. It is considered that the resulting cell structure is, to a significant extent, determined by the elongational properties of the melt. Melt properties which yielded high porosities also promoted increased cell elongation. In order to achieve foams with a very low dielectric constant, a material with lower strain hardening, such as HPE, can be used. Such a structure will likely be more difficult to achieve than the spherical structure and also likely require very well-regulated process parameters, since a difference of only a few degrees in the temperature has a great influence on the cell structure. If cell deformation is to be

avoided, a material with high strain hardening is desirable.

Adding a chemical blowing agent significantly changed the dielectric loss factor of the unexpanded grade, probably because both the blowing agent and its reactants contained permanent dipoles.

#### ACKNOWLEDGEMENTS

The authors thank Åsa Linder and Hans Eklind, both at Borealis, for supplying the compounds used in this study, also thanks to Rikard Bergman at the department of condensed matter physics for his help with dielectric measurements and discussions about properties of dielectric composites and to Professor Mikael Rigdahl for scientific guidance. Dr. J. A. Bristow is thanked for linguistic revision of the manuscript.

#### REFERENCES

1. Bur A.J. (1985), "Dielectric properties of polymers at microwave frequencies: a review", *Polymer*, **26**, 963-977.
2. Shannon, C.E. (1949), "Communication in the presence of noise", *Inst. Radio Engrs.*, **37**, 10-21.
3. Bartnikas R. and Eichhorn R.M. Ed. (1983), "Engineering dielectrics vol IIA", Pa. Cop, Philadelphia.
4. Tuncer, E. et al. (2002), "Dielectric Mixtures: Electrical properties and Modeling", *IEEE Trans. Dielec. Elec. Insul.*, **9**, 809-828.
5. Sillars, R.W. (1937), "The properties of a dielectric containing semiconducting particles of various shapes", *J. Instn. Elec. Engrs.*, **80**, 378-394.
6. Conklin, G.E. (1964), "Reduction of Dielectric Loss in Polyethylene", *J. Appl. Phys.*, **35**, 3228-3235.
7. Birk, J.B. Ed (1967), "Progress in dielectrics", Heywood, London, pp. 69-114.
8. Jonscher, A.K. (1981), "A new understanding of the dielectric relaxation of solids", *J. Mater. Sci.*, **16**, 2037-2060.
9. Baldwin, D.F. et al. (2004), "Microcellular sheet extrusion system process design models for shaping and cell growth control", *Polym. Eng. Sci.*, **38**, 674-688.
10. Klemppner D. and Frisch K. Ed. (1991), "Handbook of Polymeric Foams and Foam Technology", Hanser, Munich.
11. Cogswell, F.N. (1981), "Polymer melt rheology", George Godwin Ltd, London,.
12. Cervený S. et al. (2002), "Dielectric  $\alpha$ - and  $\beta$ -Relaxations in Uncured Styrene Butadiene Rubber", *Macromolecules*, **35**, 4337-4342.
13. Rozhkov S.S. et al. (2007), "The Electrical Properties of Schungite-Containing Compositions Based on Polypropylene and High-Density Polyethylene". *Russ. J. Phys. Chem.*, **81**, 1863-1868.
14. Acierno D. and La Mantia P. (1983), "The capability of the CEAST Capillary and Tensile Rheometer (Rheoscope 1000) to characterise Polymeric Materials", *Symp. Rheol.*, Bradford University.
15. Krause B. et al. (2002), "Ultralow-k Dielectrics Made by Supercritical Foaming of Thin Polymer Films" *Adv. Mater.*, **14**, 1041-1046.
16. Lee S.T. Ed. (2000), "Foam Extrusion - Principle and practice", Technomic Publ. Co., Lancaster, Pennsylvania,.